https://doi.org/10.15407/ujpe71.4.349

O. GNATYUK,[1] M. OLENCHUK,[1] I. KUPCHAK,[1,2] A. NIKOLENKO,[1,2]
G. DOVBESHKO,[1] E. KOVALSKA,[3] Z. SOFER[4]

[1] Institute of Physics, Nat. Acad. of Sci. of Ukraine
(46, Nauky Ave., Kyiv 03028, Ukraine)
[2] V.E. Lashkaryov Institute of Semiconductor Physics, Nat. Acad. of Sci. of Ukraine
(45, Nauky Ave., Kyiv 03028, Ukraine)
[3] University of Exeter
(North Park Road, Exeter, EX4 4QF, United Kingdom)
[4] University of Chemistry and Technology Prague
(Technická 5, 166 28 Praha 6, Czech Republic)

PHOSPHORENE AS A NEW MATERIAL FOR SURFACE-ENHANCED INFRARED SPECTROSCOPY OF CELL MEMBRANES

Phosphorene is a promising two-dimensional (2D) material consisting of a single-layer phosphorus artificially created from layered black phosphorus, which is known to be the most stable allotrope of phosphorus. Phosphorene, similar to graphene-based substrates used in surface-enhanced infrared spectroscopy (SEIRA), is expected to exhibit similar behavior. The results of a SEIRA experiment with a model biological cell membrane, formed on the basis of dioleoylphosphatidylcholine (DOPC) lipids, and deposited onto the surface of several phosphorene layers are presented. The enhancement of the absorption factor by up to 2–4 times was observed without changing the positions of the absorption frequencies of the bands corresponding to the main spectral markers of liposomes, which is comparable to that observed for metallic silver particles. Density functional theory (DFT) calculations of the DOPC-phosphorene system indicate a high reactivity of multilayer phosphorene and a possibility of the rapid, often reversible oxidation and reduction processes depending on the pH of the medium. Taking into account that the optical signal from the membrane is insignificant, this technique can be recommended for the use of two-dimensional phosphorene as SEIRA and SERS substrates for membrane studies.

K e y w o r d s: phosphorenes, spectral markers, model membranes, surface-enhanced infrared absorption.

1. Introduction

The electrical, optical, and chemical properties of two-dimensional (2D) materials are studied for many applications in the physical, chemical, biological, and medical domains, as well as in energy production and storage [1–5]. In the field of biosensor applications, 2D materials doped with metallic and non-metallic materials are used to increase the sensitivity of devices [1, 6, 7]. The application of 2D materials in biosensing is of great interest [8–10].

In the last decade, phosphorene, which is obtained from black phosphorus [5, 11], has been actively studied because of its unique optical and electrical properties [5, 12, 13]. These properties can be modified by applying mechanical stresses, electric and/or magnetic fields, defect engineering, doping, and temperature changes, as well as by varying the number of layers in the specimen [13–16].

Phosphorene is a 2D material consisting of one or more layers of black phosphorus, where the phosphorus atoms are arranged in layers and oriented perpendicular with respect to one another. Thin layers of black phosphorus exhibit semiconducting properties, a high charge carrier mobility, and a non-zero band

C i t a t i o n: Gnatyuk O., Olenchuk M., Kupchak I., Nikolenko A., Dovbeshko G., Kovalska E., Sofer Z. Phosphorene as a new material for surface-enhanced infrared spectroscopy of cell membranes. *Ukr. J. Phys.* **71**, No. 4, 349 (2026). https://doi.org/10.15407/ujpe71.4.349.

gap, which can be varied by doping and functionalization from about 1.5 eV in a monolayer to 0.3 eV in bulk phosphorus. A phosphorus atom has five electrons in the $3p$ orbitals and undergoes sp^3-hybridization. Each atom has three electrons covalently bonded to three neighboring phosphorus atoms. Each p orbital contains its own lone pair of electrons.

Due to sp^3-hybridization, phosphorenes do not have flat layers like graphene. Instead, they form folded honeycomb layers, which held together by weak van der Waals forces. The distance between the top and bottom atoms is equal to $d_1 = 2.244$ Å, and between two neighboring atoms to $d_2 = 2.224$ Å [17]. Black phosphorus has an orthorhombic crystal lattice [17], which is characterized by specific symmetry parameters for different structural forms: the base-centered orthorhombic lattice for bulk crystals, the simple orthorhombic 2D lattice for single-layer phosphorene with the symmetry group D_{2h}, an orthorhombic symmetry with the same symmetry group D_{2h} is retained as in multilayer phosphorene for the most stable AB-type packing (as in the bulk crystal).

Possessing high biocompatibility [18, 19] and unique photophysical, photochemical, and electrocatalytic properties, phosphorenes are used for applied problems in biology and medicine, in particular, in oncology for photodynamic therapy [20, 21], photothermal therapy [22, 23], and for photoimmunotherapy [24, 25], as an antibacterial agent [26, 27] in biosensorics [28, 29], and for drug delivery [30].

Based on the properties and structure of phosphorene, we predict enhanced amplification of oscillations in the SEIRA effect compared to 2D-MoS_2 or 2D-WS_2, and, in some cases, to graphene in close proximity to the inhomogeneous membrane surface. Therefore, the aim of this work is to investigate the interaction between phosphorene nanoparticles and liposomes based on dioleoylphosphatidylcholine (DOPC), as well as to analyze the possibility of enhancing absorption bands in the infrared (IR) spectra of complex biological molecules using a model cell membrane as an example.

2. Methods and Materials

To obtain phosphorene nanoparticles, we used a controlled low-potential electrochemical method of black phosphorus exfoliation in a non-aqueous, oxygen-free environment in order to produce high-quality, few-layer phosphorene with micro-scale lateral dimensions, a 100% yield, and a minimized oxidation surface. The technology was developed at the Prague University of Chemistry and Technology by the authors of Ref. [31], and the specimens were transferred to Ukraine within the framework of the Ukrainian-Czech project. Electrochemical exfoliation of black phosphorus into multilayer phosphorene was carried out in 0.01 M tetrabutylammonium hexafluorophosphate ($TBAPF_6$) in acetonitrile (AN) and 0.01-M $TBAPF_6$ in N,N-dimethylformamide (DMFA). $TBAPF_6$, as a suitable electrolyte for non-aqueous electrochemistry, was used for electrochemical exfoliation due to the chemical inertness of salt ions, which makes the electrolytic medium inert over a wide potential range. To prevent the destructive effects of oxygen and water, organic solvents with low boiling points (DMFA and AN) and a controlled oxygen-free environment created by blowing down with argon during the exfoliation process were used [31, 32].

Experimental studies were carried out using DOPC lipid (1,2-dioleoyl-sn-glycero-3-phosphocholine (850375-18:1 (Δ9-Cis) PC), Avanti Research) lipid; on its basis, liposomes, which are model membrane structures, were synthesized. First, the lipid was dissolved in chloroform and dried using nitrogen gas. After the evaporation of chloroform, a phospholipid film remained on the bottom of the flask. To exfoliate lipids from the film, distilled water was added to the flask (to form the 4 mM lipid solution), and liposomes were formed using the freeze-thaw method [33, 34]. The freezing procedure, subsequent thawing at room temperature, and ultrasonic treatment for 1 min before the next freezing were carried out three times. After the formation of liposomes, DOPC solutions of phosphorene nanoparticles with concentrations of 1.5 mg/ml (specimen 1) and 1.3 mg/ml (specimen 2) were added to the liposomes, and the spectral changes in the IR spectrum were analyzed. This method of forming liposomes with nanoparticles was tested, and the results were presented in Refs. [35, 36], where data on the enhancement or attenuation of oscillations in the spectra of liposomes with other 2D materials, such as MoS_2 and WS_2, were also presented.

The study of phosphorene was performed using Raman and infrared (IR) spectroscopy. Raman spectra were registered at room temperature in the backscat-

tering configuration using a T-64000 Horiba Jobin-Yvon Raman spectrometer with a triple monochromator. The spectrometer was equipped with an electrically cooled silicon CCD detector and an Olympus BX41 microscope. A laser line with a wavelength of 488 nm from an Ar–Kr ion laser was used for excitation. The excitation radiation was focused on the specimen surface using an optical objective ×50/NA 0.75, which provided a laser spot of about 1 μm in diameter. The laser beam power at the specimen surface was varied within the range of 0.1–5 mW.

The IR spectroscopy method was used to study and analyze the interaction between phosphorene and liposomes and the enhancement of oscillations in the liposome spectra. The IR spectra of the examined phosphorene specimens were registered on an INVENIO-R spectrometer (Bruker, Germany) in transmission mode. For this purpose, phosphorene specimens, which were previously prepared in dimethyl sulfoxide (DMSO), were deposited onto IR-transparent CaF_2 substrates and dried at room temperature. After registering the spectra, a baseline correction was performed. The spectra were processed using the OPUS 4.0 software. A BioATRCell II accessory was also used to register spectra. This attenuated total reflectance (ATR) accessory for the Fourier transform infrared (FTIR) spectrometer INVENIO-R was designed to study the spectra of aqueous solutions and suspensions in water.

Theoretical studies of the interaction between phosphorene and a lipid fragment were carried out using first-principles calculations based on density functional theory (DFT) to predict the properties of phosphorene-based nanomaterials.

3. Experimental Results

3.1. Raman scattering spectra of phosphorene

Three main modes of phosphorene were observed in the experimental spectra, namely, A_g^1, B_{2g}, and A_g^2. According to their position, we can assert that the studied phosphorene specimens contained a few (3–5) layers [37].

Although the phosphorene concentrations in the specimens did not differ much (specimen 1 had a concentration of 1.5 mg/ml, and specimen 2 a concentration of 1.3 mg/ml), this difference significantly affected the appearance of their Raman scattering spectra. In the case with a higher phosphorene concentration, we observed an atypical for multilayer phosphorene distribution of the intensities of the three main modes A_g^1, B_{2g}, and A_g^2; namely, mode B_{2g} had the highest intensity. At the same time, for the specimen with a lower phosphorene concentration, the distribution of intensities and the positions of the main modes A_g^1, B_{2g}, and A_g^2 corresponded to phosphorene specimen with a thickness of 3–5 layers (Fig. 1). It can be assumed that as the phosphorene concentration increased, the processes of phosphorene aggregation and oxidation may occur.

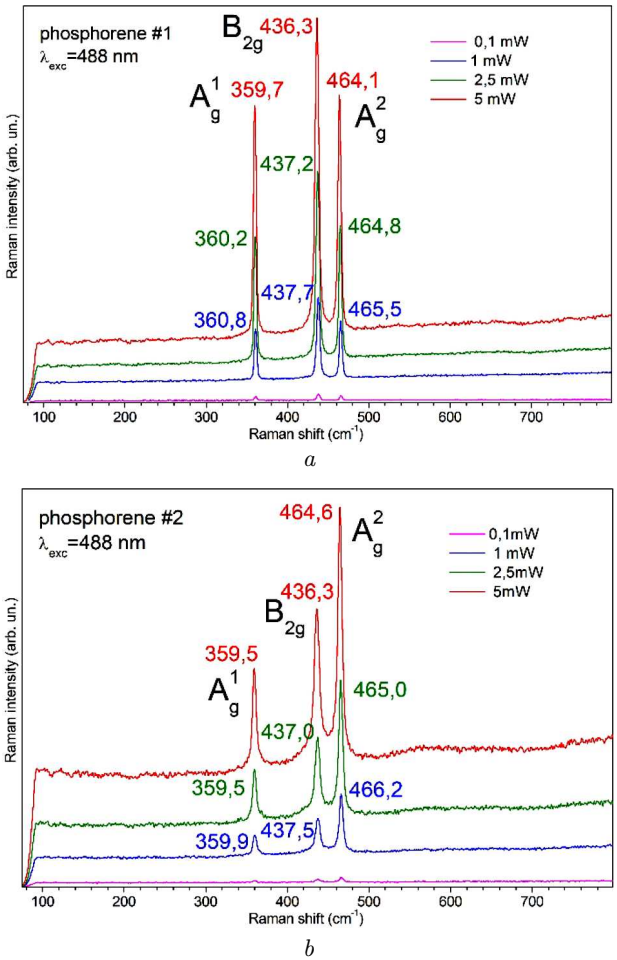

Fig. 1. Raman spectra of phosphorene with various concentrations: 1.5 (*a*) and 1.3 mg/ml (*b*)

3.2. Infrared spectra of phosphorene

Specimens of phosphorene dispersed in DMSO with phosphorene concentrations of 1.5 mg/ml (speci-

Table 1. **Identification of vibrational modes for phosphorene specimens in DMSO**

Phosphorene specimen	NH	CH ring	CH_2 str.	CH_2 str	C=O	C–N	CH def.	sym. PO_2^-	C–O
Phosphorene 1	3227	3053	2916	2850	1734	1627	1458	1184	944
Phosphorene 2	3201	3053	2916	2850	1734	1600	1439	1157	934

men 1) and 1.3 mg/ml (specimen 2) were used in the experiment. In this case, DMSO played the role of a non-polar hydrophobic solvent, which protected phosphorene from oxidation.

According to the frequency positions (Fig. 2), it can be noted that in the case of a lower phosphorene concentration (specimen 2), some bands are located at lower frequencies. The fact that we registered bands in the region around 1734 cm^{-1}, which is attributed to the C=O bond, and in the region at 1184 (for specimen 1) or 1157 cm^{-1} (for specimen 2), which is associated with the symmetric stretching vibrations of the molecular group PO_2, may indicate that during the air drying process, an oxidation process occurs, which is undesirable for the examined specimens. We also registered the bands of stretching vibrations of molecular groups CH_2, NH, C–N, CH deformation, and C–O, which are not characteristic of the DMSO solvent based on their positions, but may be partially associated with its presence and modified due to interaction with phosphorene. The most

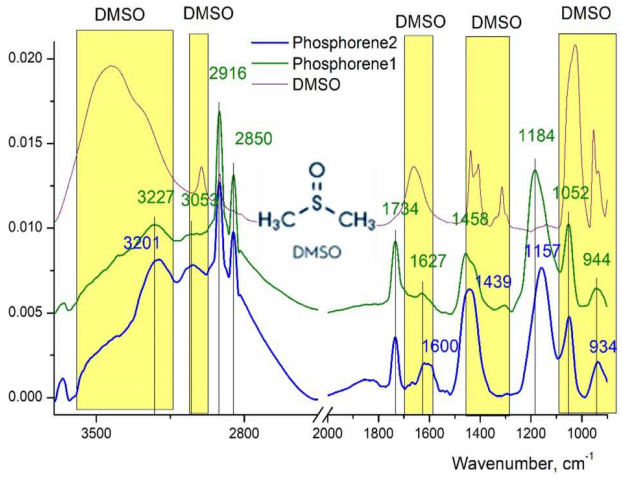

Fig. 2. IR absorption spectra of phosphorene with various concentrations: 1.5 (Phosphorene 1) and 1.3 mg/ml (Phosphorene 2). The yellow color indicates the absorption ranges of DMSO. The specimen with a higher concentration is more highly oxidized

intense absorption band of DMSO, namely S=O, is at 1025 cm^{-1}. In addition, characteristic features are absorption bands of stretching vibrations $-CH_3$ at 3001 and 2917 cm^{-1} associated with the S atom, as well as deformation vibrations of the same molecular groups at 1437, 1406, and 1314 cm^{-1}. The bands at 953 and 933 cm^{-1} can be attributed to the C–O absorption.

3.3. Infrared spectra of liposomes with phosphorene

The experimental spectrum of liposomes with DOPC has characteristic features indicating the successful formation of liposomes (Fig. 3, Table 2). These are the bands in the hydrogen bond absorption region; namely, the OH stretching vibration band at 3400 cm^{-1}, the OH deformation vibration band at 1640 cm^{-1}, and a characteristic hydrogen bond absorption interval in the region of phosphate groups at 1100–1000 and 820 cm^{-1}. The DOPC phospholipid is characterized by the presence of a C=C double bond. An interval of 3006–2700 cm^{-1} is associated with the stretching vibrations of the molecular groups CH_2 and CH_3, and it is a conformational feature of phospholipid tails. The presence of the C=O group is demonstrated by a characteristic absorption band at 1736 cm^{-1}. Also characteristic and conformationally sensitive are the bands in an interval of 1240–1220 cm^{-1} (the asymmetric vibration of PO_2^-) and at 1090 cm^{-1} (the symmetric vibration of PO_2^-).

For complexes with phosphorenes, we achieved an enhancement of the main vibrational modes of liposomes by 2–4 times, and the enhancement factor was larger for the specimen with a lower phosphorene concentration (Table 3). No frequency shifts of the absorption bands of liposomes were observed.

When comparing the IR absorption spectra of phosphorene and DMSO, it is possible to distinguish intervals where the solvent may give an additive contribution. However, in this case, those contributions

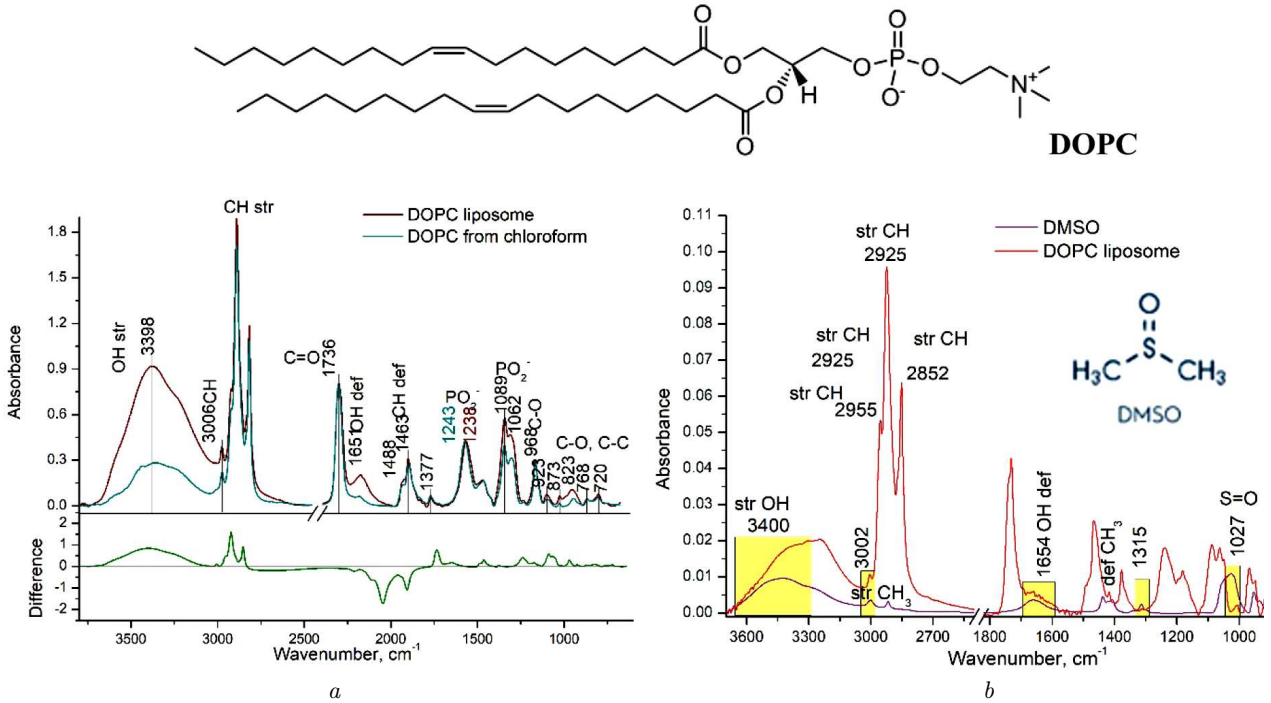

Fig. 3. IR absorption spectra of liposomes with DOPC and pure DOPC deposited from chloroform (*a*). IR absorption spectra of liposomes with DOPC and DMSO (*b*). The selected area indicates the absorption intervals of DMSO; when calculating the enhancement factors in these ranges, the additive contribution of DMSO should be taken into account

are insignificant or do not overlap with the absorption bands of liposomes (Fig. 3, *b*). Generally speaking, in the case of using phosphorene as a substrate for an enhancement the optical signal from other molecules, and the influence of phosphorene can distort the IR spectrum more strongly, it is desirable to purify phosphorene from the solvent by filtration.

In the case where phosphorene interacts with liposomes, two processes can be pointed out. One of them is the enhancement of absorption bands, with practically no change in the positions of main bands (Table 2). This process is observed within the interval of CH stretching and deformation vibrations, as well as for C=O stretching vibrations. Moreover, a characteristic feature is that for the lower phosphorene concentration, we observe a larger enhancement (by 4.1–4.8 times) than for the higher phosphorene concentration (by 1.6–2.7 times). The other process is the appearance of a new intense band at 1240 cm^{-1}, which may be associated with the process of phosphorene interaction with phospholipid heads, as well as with the oxidation of phosphorene in an aqueous environment. The band at

Table 2. **Identification of vibrational modes for phosphorene specimens with DOPC liposomes**

DOPC liposomes	DOPC liposomes + Phosphoren 1 = = 1.5 mg/ml	DOPC liposomes + Phosphoren 2 = = 1.3 mg/ml	Identification of vibrations
3400	3400	3400	str. OH
3243	3243	3243	str. NH
3004	3004	3004	str. CH ring
2955	2955	2955	str. C–H_3
2925	2925	2925	str. C–H_2
2880	2880	2880	str. C–H_3
2852	2852	2852	str. C–H_2
1732	1732	1732	str. C=O
1658	1658	1658	str. C=C, def. OH
1467	1467	1467	def. C–H_2
1377	1377	1377	def. C–H_3
1239	1239	1239	str. PO_2^- asym.
1182	1182	1182	C–O
1087	1087	1087	str. PO_2^- sym.
1062	1062	1062	C–O–PO_2^-
970	970	970	C–O, C–N–C

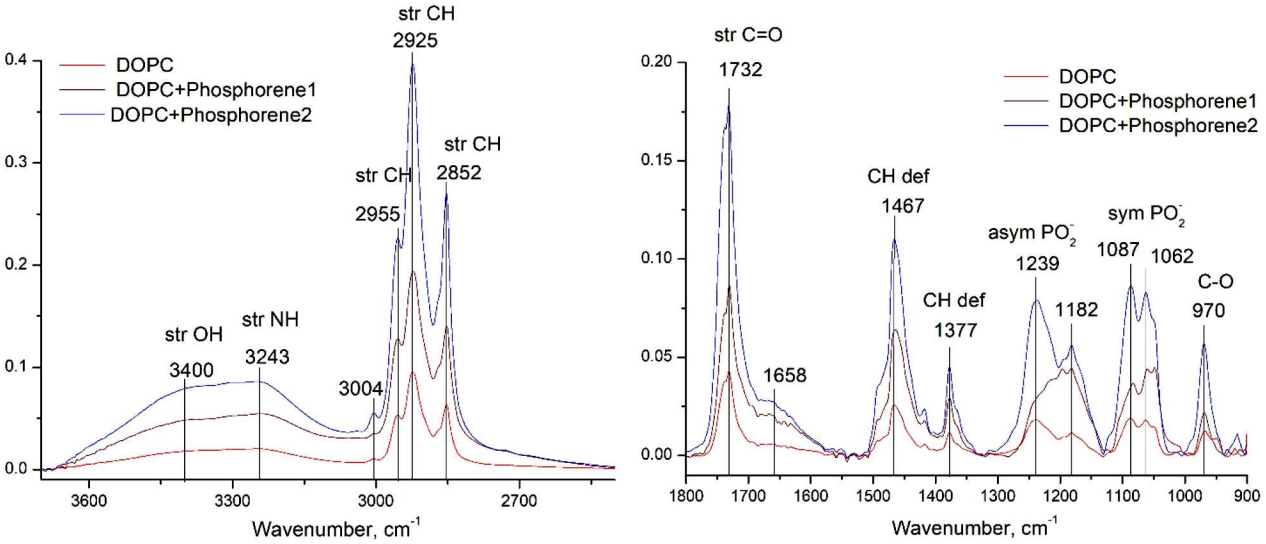

Fig. 4. IR absorption spectra of liposomes with DOPC and phosphorene of different concentrations. Phosphorene 1 = = 1.5 mg/ml, Phosphorene 2 = 1.3 mg/ml

Table 3. **Enhancement coefficients of the main absorption bands of phosphorene with liposomes**

Phosphorene specimen	OH*	NH	CH	CH	CH	C=O*	CH def.	asym. PO_2^-	sym. PO_2^-	C–O*
Phosphorene 1	2.7	2.6	2.4	2.2	2.2	2.0	2.5	1.6	1.9	1.8
Phosphorene 2	4.4	4.1	4.2	4.1	4.2	4.1	4.3	4.4	4.5	4.8

* DMSO absorption and phosphorene oxidation may contribute to these bands.

1182 cm^{-1} most likely reflects the additive contribution of phosphorene absorption.

3.4. Quantum-chemical calculations

Calculations of the interaction of DOPC lipid with a phosphorene nanoparticle (P) were performed using the density functional theory (DFT) method implemented in the GAMESS-US software package [39, 40]. The exchange-correlation interaction was described by the hybrid functional B3LYP [41], which includes a part of the exact Hartree–Fock exchange and thus makes it possible to obtain a band gap value close to the experimental one. Together with the set of basis functions and effective nuclear potentials LANL2DZ [42–44], this approach allows the energy spectra of systems containing hundreds of atoms to be calculated with good accuracy. The van der Waals interaction was consistently taken into account by including the DFT-D3 functional [45]. Geometry optimization of all studied systems was carried out over all internal variables and without using symmetry operations until the largest component of the potential energy gradient of the system became less than 10^{-4} a.u.

The phosphorene nanoparticle was simulated as a please make 32 and 14 as subscripts cluster, where the broken bonds at the edges were passivated by hydrogen atoms. During the optimization process without imposed symmetry constraints, such a cluster retains the "armchair" configuration, with a bond length of 2.45 Å in the "armchair" direction, and 2.42 Å in the "zigzag" one. Calculations of the density of states (DOS) for the optimized cluster showed an empty band gap with a width of about 3 eV, which indicates the complete absence of surface (defect) states.

Having constructed an optimized cluster, we analyzed its oxidation process. For this purpose, two approaches were considered: (i) oxidation of phos-

phorene by an oxygen atom =O and (ii) its oxidation by the hydroxyl group OH^-. Instead of a hydrogen atom, the relevant group was attached to one of the terminal phosphorus atoms, and the geometry optimization was performed. Generally speaking, oxidation is an expected phenomenon because the triply coordinated phosphorus atoms in phosphorene are bound by the sp^3-hybridized electron pairs, and the "extra" pair of electrons allows the formation of the double bond of the oxygen atom =O, whereas the hydroxyl group $–OH^-$ lacks one electron for a full-value bond. As a result, our calculations showed that the energy of the double bond with oxygen is about −17 eV, which is two orders of magnitude higher than that for the hydroxyl group. In turn, contains eight oxygen atoms in the DOPC molecule: two atoms in the oleic groups, which have a bound charge of 2 electrons, and 4 atoms in the phosphate group, two of which are bound only to the phosphorus atom, but have a charge of 1.5 electrons. Thus, in order to study the possibility of phosphorene oxidation by a DOPC lipid molecule, we selected the oxygen atom in the oleic group, which forms a double bond with the carbon atom.

The optimized phosphorene cluster was placed near the lipid molecule in such a way that the oxygen atom with the P=O bond replaced the oxygen atom in the C=O bond of the oleic group; then, the entire system was relaxed. However, during the relaxation process, the oxygen-cluster bonds were reconstructed, which led to the complete repulsion of the cluster from the lipid molecule: the distance between the oxygen and the nearest phosphorus atom increased to 3.2 Å, which corresponds to characteristic distances for weak interaction via van der Waals forces. The binding energy

$$E_b = E_{\text{DOPC+P}} - E_{\text{DOPC}} - E_{\text{P}}$$

was equal to −0.232 eV, which is typical of van der Waals interaction. No appreciable changes in the geometric structure of the lipid or the cluster were observed, despite the fact that a broken bond appeared at the terminal phosphorus atom.

At the next stage, we checked whether the pH level affects the phosphorene oxidation by the DOPC lipid. We considered a situation in which a neutral lipid is immersed into a solution that contains phosphorene particles and is characterized by a certain pH level. We repeated the above procedure for the systems

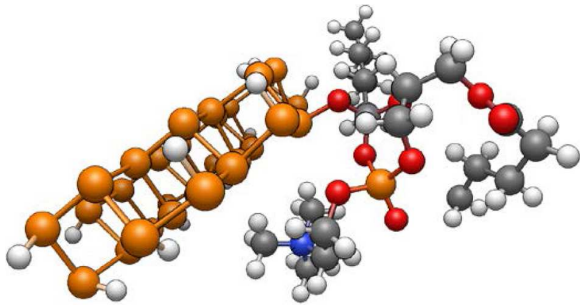

Fig. 5. Schematic diagram of a DOPC lipid bound to a phosphorene cluster. The atoms are colored as follows: P (brown), C (gray), O (red), N (blue), and H (white). The bond between the phosphorus and oxygen atoms of the oleic group can be observed. Some parts of the oleic acid chains are not shown

charged to $+1e$ (an acidic medium, in which the system gives up a negative charge to H^+) and $-1e$ (an alkaline medium, in which the system gives up a positive charge to OH^-). The initial geometric configuration of the atoms was the same as in the neutral system.

During the relaxation process, it turned out that the alkaline medium did not affect the oxidation process: in the negatively charged system, the phosphorene cluster separated from the lipid as in the case of a neutral system; the distance turned out to be 3.2 Å as well, and the binding energy was −0.134 eV. However, the situation was drastically different for the positively charged system. In this case, a substantial deformation of the lipid molecule was observed. As a result, one oxygen atom from the phosphate group became bound to the carbon atom in the oleic group that was connected to the phosphorene. In this case, the bond between the oxygen atom and the phosphorene was preserved, and its length was 1.793 Å, which is somewhat longer than the longest P–O bond in the phosphate group (1.730 Å). The corresponding bond energy turned out to be the lowest, reaching −3.6 eV, which considerably exceeds typical values for van der Waals bonds. The optimized structure of the DOPC lipid molecule with a phosphorene particle is shown in Fig. 5. For simplicity, some parts of the "tails" are not shown, but they were taken into account in the calculations. Figure 5 clearly demonstrates the characteristic structure of phosphorene, as well as the bond between the phosphate oxygen and the carbon of the oleic group. The other "tail" remains unchanged, although its position relative to other structural parts of the lipid is altered.

Finally, it is important to determine whether the process of phosphorene oxidation by the oxygen-containing group of the lipid is reversible. For this purpose, we optimized the geometry of the lipid–phosphorene system, proceeding from the optimized positively charged structure.

Hence, if the positive charge changes to neutral or negative, the system still remains bound, although it becomes substantially deformed. The deformation mainly manifests itself in the reorientation of the "tails", whereas the bond between the phosphate and oleic groups remains in any charge state. It is worth noting that if the oxidized system is transferred to an alkaline medium, where it obtains a charge of $-1e$, the binding energy drastically decreases to +0.3 eV, i.e., oxidation with an additional O–C bond is impossible in such a configuration without an external influence, whereas the reduction reaction is potentially possible. In a neutral medium, the binding energy becomes two times higher (−0.6 eV), which excludes the phosphorene reduction.

On the basis of the results of quantum-chemical calculations, it can be concluded that the absorption enhancement phenomenon in the particle–DOPC system can include both chemical and electromagnetic mechanisms. These are

1) the charge transfer between the molecule and the nanostructure during the oxidation-reduction process, which becomes stronger under optical excitations and as a result of the increase in the molecular dipole moment;

2) the appearance of additional local electromagnetic fields at the inhomogeneous structures on the complicated surface of liposomes when exciting light interacts with the electronic states of phosphorenes.

4. Conclusions

A new material, few-layer (3–5 layers) phosphorene in the form of a suspension of nanoparticles and films, has been characterized using vibrational spectroscopy. The technology for obtaining liposome specimens with phosphorene nanoparticles on their surface has been developed.

The marker bands of phosphorenes in the suspension have been identified, the influence of the solvent on the IR spectra of phosphorenes has been estimated, and the purification of phosphorenes from impurities for precision measurements has been proposed.

The interaction of phosphorene with model DOPC-based membranes has been studied using FTIR spectroscopy. It was shown that due to this interaction, the optical signal can be amplified by a factor of 1.6–4.8, with the enhancement factor being larger for phosphorene at lower concentrations. The enhancement coefficient in this system is an order of magnitude higher than that for WS_2 and MoS_2 layers (30–50%), and higher than that for colloidal silver particles in a similar system (of about 3).

Quantum-chemical calculations have shown the possibility of oxidation-reduction resulting to deformation of lipid molecule in the case of the model DOPC lipid molecule on a single phosphorene layer. The inhomogeneous charge distribution over the surface of a lipid macromolecule or a liposome can modulate the electron concentration in various molecular groups and parts of the phosphorene layer, which will lead to the appearance of local fields and, as a result, to the redistribution of the optical response for a liposome near the nanoparticles.

1. A.H. Khan, S. Ghosh, B. Pradhan, A. Dalui, L.K. Shrestha, S. Acharya, K. Ariga. Two-dimensional (2D) nanomaterials towards electrochemical nanoarchitectonics in energy-related applications. *Bull. Chem. Soc. Jpn.* **90**, 627 (2017).
2. A.V. Terebilenko, M.V. Olenchuk, D.O. Mazur, A.S. Nikolenko, V.I. Popenko, G.I. Dovbeshko, O. Bezkrovnyi, T. Sabov, B.M. Romanyuk, V.N. Poroshin, S.V. Ryabukhin, D.M. Volochnyuk, S.V. Kolotilov. Influence of formation temperature on the morphology of MoS_2 and its catalytic properties in the hydrogenation of isomeric bromoquinolines to bromo-1,2,3,4-tetrahydroquinolines. *Dalton Trans.* **54**, 13057 (2025).
3. M.V. Olenchuk, U.K. Afonina, O.P. Gnatyuk, V.V. Strelchuk, A.S. Nikolenko, G.I. Dovbeshko. Heat annealing influences the optical properties of 2D-MoS_2 nanoparticles. *Mol. Cryst. Liq. Cryst.* **749**, 1 (2022).
4. G.I. Dovbeshko, U.K. Afonina, M.V. Olenchuk, I.M. Kupchak, O.P. Gnatyuk, G.P. Monastyrskyi, A.S. Nikolenko, H.V. Shevliakova, A.N. Morozovska. Effect of 2D-WS_2 nanoparticles on a local electrical field at a membrane vicinity: Vibrational spectroscopy data. *J. Phys. Chem. C* **128**, 1131 (2024).
5. V. Sorkin, Y. Cai, Z. Ong, G. Zhang, Y.W. Zhang. Recent advances in the study of phosphorene and its nanostructures. *Crit. Rev. Solid State Mater. Sci.* **42**, 1 (2017).
6. S.M. Tan, M. Pumera. Two-dimensional materials on the rocks: Positive and negative role of dopants and impurities in electrochemistry. *ACS Nano* **13**, 2681 (2019).
7. J. Chao, M. Zou, C. Zhang, H. Sun, D. Pan, H. Pei, S. Su, L. Yuwen, C. Fan, L.A. Wang. A MoS_2-based system for

efficient immobilization of hemoglobin and biosensing applications. *Nanotechnology* **26**, 274005 (2015).
8. C.I. Idumah. Phosphorene polymeric nanocomposites for biomedical applications: A review. *Int. J. Polym. Mater. Polym. Biomater.* **73,** 292 (2024).
9. K.H. Min, K.H. Kim, S.P. Pack. Two-dimensional materials for biosensing: Emerging bio-converged strategies for wearable and implantable platforms. *Chemosensors* **13**, 209 (2025).
10. J. Ko, C. Ock, H. Gim, K. Hong, Y. Lee, K.C. Kwon. Two-dimensional materials for artificial sensory devices: Advancing neuromorphic sensing technology. *npj 2D Mater. Appl.* **9**, 35 (2025).
11. R. Gusmão, Z. Sofer, M. Pumera. Black phosphorus rediscovered: From bulk material to monolayers. *Angew. Chem. Int. Ed. Engl.* **56**, 8052 (2017).
12. R.K. Mishra, J. Sarkar, I. Chianella, S. Goel, H.Y. Nezhad. Black phosphorus: The rise of phosphorene in 2D materials applications. *Next Materials* **4**, 100217 (2024).
13. A. Chalechale, R. Melnik, Z.L. Miškovic. Modeling of anisotropy effects in phosphorene devices. *Phys. Rev. Appl.* **23**, 064031 (2025).
14. M.S. Islam, M.T. Islam, M.R. Hossain. Phosphorene: A novel nanomaterial revolutionizing biomedicine. *JCIS Open* **16**, 100123 (2024).
15. A. Jain, A. McGaughey. Strongly anisotropic in-plane thermal transport in single-layer black phosphorene. *Sci. Rep.* **5**, 8501 (2015).
16. X. Zhang, Q. Li, B. Xu, B. Wan, J. Yin, X.G. Wan. Tuning carrier mobility of phosphorene nanoribbons by edge passivation and strain. *Phys. Lett. A* **380**, 614 (2016).
17. L. Kou, C. Chen, S.C. Smith. Phosphorene: fabrication, properties, and applications. *J. Phys. Chem. Lett.* **6**, 2794 (2015).
18. N.M. Latiff, C.C. Mayorga-Martinez, Z. Sofer, A.C. Fisher, M. Pumera. Cytotoxicity of phosphorus allotropes (black, violet, red). *Appl. Mater. Today* **13**, 310 (2018).
19. M. Qiu, A. Singh, D.Wang, J. Qu, M. Swihart, H. Zhang, P.N. Prasad. Biocompatible and biodegradable inorganic nanostructures for nanomedicine: Silicon and black phosphorus. *Nano Today* **25**, 135 (2019).
20. J. Ouyang, Y. Deng, W. Chen, Q. Xu, L. Wang, Z. Liu, F. Tang, L. Deng, Y.N. Liu. Marriage of artificial catalase and black phosphorus nanosheets for reinforced photodynamic antitumor therapy. *J. Mater. Chem. B* **6**, 2057 (2018).
21. J. Liu, P. Du, T. Liu, B.J. Córdova Wong, W. Wang, H. Ju, J. Lei. A black phosphorus/manganese dioxide nanoplatform: Oxygen self-supply monitoring, photodynamic therapy enhancement and feedback. *Biomaterials* **192**, 179 (2019).
22. J. Xie, T. Fan, J.H. Kim, Y. Xu, Y. Wang, W. Liang, L. Qiao, Z. Wu, Q. Liu, W. Hu, N. Yin, L. Yang, L. Liu, J.S. Kim, H. Zhang. Large-area flexible organic solar cells with a robust silver nanowire-polymer composite as transparent top electrode. *Adv. Funct. Mater.* **30**, 1 (2020).
23. G. Yang, X. Wan, Z. Gu, X. Zeng, J. Tang. Near infrared photothermal-responsive poly(vinyl alcohol)/black phosphorus composite hydrogels with excellent on-demand drug release capacity. *J. Mater. Chem. B* **6**, 1622 (2018).
24. M.A. Buabeid, E.S.A. Arafa, G. Murtaza, Emerging prospects for nanoparticle-enabled cancer immunotherapy. *J. Immunol. Res.* **2020**, 9624532 (2020).
25. X. Shou, Y. Liu, D. Wu, H. Zhang, Y. Zhao, W. Sun, X. Shen. Black phosphorus quantum dots doped multifunctional hydrogel particles for cancer immunotherapy. *Chem. Eng. J.* **408**, 127349 (2021).
26. Z.L. Shaw, S. Kuriakose, S. Cheeseman, E.L.H. Mayes, A. Murali, Z.Y. Oo, T. Ahmed, N. Tran, K. Boyce, J. Chapman, C.F. McConville, R.J. Crawford, P.D. Taylor, A.J. Christofferson, V.K. Truong, M.J.S. Spencer, A. Elbourne, S. Walia. Broad-spectrum solvent-free layered black phosphorus as a rapid action antimicrobial. *ACS Appl. Mater. Interfaces* **13**, 17340 (2021).
27. P. Zhang, B. Sun, F. Wu, Q. Zhang, X. Chu, M. Ge, N. Zhou, J. Shen. Wound healing acceleration by antibacterial biodegradable black phosphorus nanosheets loaded with cationic carbon dots. *J. Mater. Sci.* **56**, 6411 (2021).
28. Ying Teng Yew, Z. Sofer, C.C. Mayorga Martinez, M. Pumera. Black phosphorus nanoparticles as a novel fluorescent sensing platform for nucleic acid detection. *Mater. Chem. Front.* **1**, 1130 (2017).
29. V. Kumar, J.R. Brent, M. Shorie, H. Kaur, G. Chadha, A.G. Thomas *et al.* Nanostructured aptamer-functionalized black phosphorus sensing platform for label-free detection of myoglobin, a cardiovascular disease biomarker. *ACS Appl. Mater. Interfaces* **8**, 22860 (2016).
30. W. Chen, J. Ouyang, H. Liu, M. Chen, K. Zeng, J. Sheng, Z. Liu, Y. Han, L. Wang, J. Li, L. Deng, Y.-N. Liu, S. Guo. Black phosphorus nanosheet-based drug delivery system for synergistic photodynamic/photothermal/chemotherapy of cancer. *Adv. Mater.* **29**, 1603864 (2017).
31. E. Kovalska, J. Luxa, T. Hartman, N. Antonatos, P. Shaban, E. Oparin, M. Zhukova, Z. Sofer. Non-aqueous solution-processed phosphorene by controlled low-potential electrochemical exfoliation and thin film preparation. *Nanoscale* **12**, 2638 (2020).
32. P. Yasaei, B. Kumar, T. Foroozan, C. Wang, M. Asadi, D. Tuschel, J.E. Indacochea, R.F. Klie, A. Salehi-Khojin. High-quality black phosphorus atomic layers by liquid-phase exfoliation. *Adv. Mater.* **27**, 1887 (2015).
33. M. Bogdanov, K. Pyrshev, S. Yesylevskyy, S. Ryabichko, V. Boiko, P. Ivanchenko, R. Kiyamova, Z. Guan, C. Ramseyer, W. Dowhan. Phospholipid distribution in the cytoplasmic membrane of Gram-negative bacteria is highly asymmetric, dynamic, and cell shape-dependent. *Sci. Adv.* **6**, eaaz6333 (2020).
34. G.I. Dovbeshko, U.K. Afonina, M.V. Olenchuk, I.M. Kupchak, O.P. Gnatyuk, G.P. Monastyrskyi, A.S. Nikolenko, H.V. Shevliakova, A.N. Morozovska. Effect of 2D-WS_2 nanoparticles on a local electrical field at a membrane vicini-

ty: Vibrational spectroscopy data. *J. Phys. Chem. C* **128**, 1131 (2023).
35. G. Monastyrskyi, O. Gnatyuk, I. Gubareni, G. Levchenko, A. Nikolenko, M. Olenchuk, A. Tolochko, I. Kupchak, G. Dovbeshko. MoS_2 2D nanoparticles as inducers of changes in liposomes formation and their spectroscopic properties. *Low Temp. Phys.* **51**, 261 (2025).
36. M. Olenchuk, G. Monastyrskyi, Yu.M. Barabash, O. Gnatyuk, Ie. Gubareni, G. Levchenko, A. Nikolenko, A. Tolochko, I. Kupchak, G. Dovbeshko. The influence of 2D WS_2 nanoparticles on the liposomes formation, morphology and spectral properties. *J. Molecul. Struct.* **1352**, Part 1, 144277 (2025).
37. Z. Guo, H. Zhang, S. Lu, Z. Wang, S. Tang, J. Shao, Z. Sun, H. Xie, H. Wang, X.-F. Yu, P.K. Chu. From black phosphorus to phosphorene: Basic solvent exfoliation, evolution of raman scattering, and applications to ultrafast photonics. *Adv. Funct. Mater.* **25**, 6996 (2015).
38. J. Gómez-Pérez, B. Barna, I.Y. Tóth, Z. Kónya, Á. kos Kukovecz. Quantitative tracking of the oxidation of black phosphorus in the few-layer regime. *ACS Omega* **3**, 12482 (2018).
39. *GAMESS-US, version 15 JUL 2024 (R2 Patch 1).*
40. G.M.J. Barca, C. Bertoni, L. Carrington *et al.* Recent developments in the general atomic and molecular electronic structure system. *J. Chem. Phys.* **152**, 154102 (2020).
41. P.J. Stephens, F.J. Devlin, C.F. Chabalowski, M.J. Frisch. *Ab initio* calculation of vibrational absorption and circular dichroism spectra using density functional force fields. *J. Phys. Chem.* **98**, 11623 (1994).
42. P.J. Hay, W.R. Wadt. *Ab initio* effective core potentials for molecular calculations. Potentials for the transition metal atoms Sc to Hg. *J. Chem. Phys.* **82**, 270 (1985).
43. W.R. Wadt, P.J. Hay. *Ab initio* effective core potentials for molecular calculations. Potentials for main group elements Na to Bi. *J. Chem. Phys.* **82**, 284 (1985).
44. P.J. Hay, W.R. Wadt. Ab initio effective core potentials for molecular calculations. Potentials for K to Au including the outermost core orbitals. *J. Chem. Phys.* **82**, 299 (1985).
45. S. Grimme, J. Antony, S. Ehrlich, H. Krieg. A consistent and accurate ab initio parametrization of density functional dispersion correction (DFT-D) for the 94 elements H–Pu. *J. Chem. Phys.* **132**, 154104 (2010).

Received 25.12.25.
Translated from Ukrainian by O.I. Voitenko

О. Гнатюк, М. Оленчук,
І. Купчак, А. Ніколенко, Г. Довбешко,
Є. Ковальська, З. Софер

ФОСФОРЕНИ ЯК НОВИЙ МАТЕРІАЛ ДЛЯ ПОВЕРХНЕВО-ПІДСИЛЕНОЇ ІНФРАЧЕРВОНОЇ СПЕКТРОСКОПІЇ КЛІТИННИХ МЕМБРАН

Фосфорен – це перспективний двовимірний матеріал, що складається з моношару фосфору, штучно створеного з шаруватого чорного фосфору, відомого як найстабільніший алотроп фосфору. Ми очікуємо, що фосфорени демонструватимуть подібну поведінку до графенових підкладок для поверхнево-посиленої інфрачервоної спектроскопії (SEIRA). В даній роботі представлено експеримент SEIRA на модельній біологічній клітинній мембрані на основі ліпідів DOPC на поверхні з кількох шарів фосфорену. Коефіцієнт підсилення, отриманий в експерименті, становить до 2–4 без зміни положень частот поглинання основних маркерних смуг ліпосом, що можна порівняти з даними на частинках металевого срібла. DFT-розрахунки системи DOPC-фосфорен показали високу реакційну здатність багатошарових фосфоренів і можливість швидкого, часто оборотного, залежно від pH середовища, окислення й відновлення фосфорену ліпідними групами. Враховуючи, що оптичний сигнал від мембрани незначний, цю методику можна рекомендувати для експериментів із застосуванням 2D-фосфорену як підкладки SEIRA та SERS у дослідженні мембран.

Ключові слова: фосфорени, спектральні маркери, модельні мембрани, поверхнево-підсилене інфрачервоне поглинання (SEIRA).